

# Adaptive N-Mesoionic Ligands Anchored to a Triazolylidene for Ruthenium-Mediated (De)Hydrogenation Catalysis

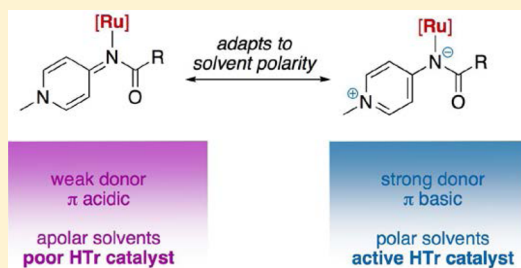
Kate F. Donnelly,<sup>†</sup> Candela Segarra,<sup>†,‡</sup> Li-Xiong Shao,<sup>†</sup> Rachele Suen,<sup>†</sup> Helge Müller-Bunz,<sup>†</sup> and Martin Albrecht<sup>\*,†,‡</sup>

<sup>†</sup>School of Chemistry and Chemical Biology, University College Dublin, Belfield, Dublin 4, Ireland

<sup>‡</sup>Department of Chemistry and Biochemistry, Universität Bern, Freiestrasse 3, 3012 Bern, Switzerland

## Supporting Information

**ABSTRACT:** A ruthenium cymene complex bearing a bidentate ligand composed of the N-mesoionic donor *N*-[1-methylpyridin-4(1*H*)-ylidene]-amide and the C-mesoionic donor 1,2,3-triazolylidene was prepared. Spectroscopic analyses including UV–vis, electrochemical, and NMR methods demonstrate that the pyridylideneamide ligand adapts to its environment and switches, depending on the solvent, between a formally anionic and a neutral donor. A mesoionic pyridinium-amidate structure predominates in polar solvents, whereas a neutral pyridylidene imine structure prevails in apolar solvents. The implications of these solvent-dependent electronic characteristics have been exploited in redox catalysis involving alcohol dehydrogenation and transfer dehydrogenation. The results indicate that the ligand resonance flexibility provides a new approach to enhance catalytic performance.



## INTRODUCTION

Homogeneous catalysis with transition metals depends critically on the availability of enabling ligands that ideally enhance the catalytic activity and impart high selectivity by substrate recognition or by shaping the catalytic cavity.<sup>1</sup> Significantly, specific properties may facilitate one step in a catalytic cycle, yet inhibit another one, which may lead to a seemingly counter-intuitive effect, as elaborated for example in the Curtin–Hammett principle.<sup>2</sup> Thus, static ligands may have severe limitations for the design of efficient homogeneous catalysts. More recent work has thus focused on the exploitation of noninnocent ligands that alter their structure and function during the catalytic cycle.<sup>3</sup> These alterations classically involve either electron transfer (redox-active ligands),<sup>4</sup> proton transfer,<sup>5</sup> or a combination of both, viz., proton-coupled electron transfer (PCET) processes.<sup>6</sup> A hallmark example is Noyori's diene ruthenium catalyst, which swaps between an anionic amide and a neutral amine donor in the catalytic cycle, depending on the presence of either a substrate or a hydrogen donor.<sup>7</sup> Similar effects have been induced by a variety of motifs, including among others de- and rearomatization,<sup>8</sup> proton transfer to pH-sensitive ligand sites,<sup>9</sup> and single-electron transfers to ligand units.<sup>10</sup> These ligands display varying degrees of donor ability toward the metal center and reveal thus a flexible electronic character, which is particularly attractive for the stabilization of several intermediates throughout the catalytic cycle by promoting for example oxidative addition (e.g., as formally anionic strong donors) and reductive elimination (in formally neutral weaker donor form). This switchable and dynamic ligand bonding has great potential, as the ligand may adapt to

the requirements of the metal at any given stage of the catalytic cycle.

Here we demonstrate the catalytic implications of a different type of ligand switchability that is based on resonance structure modulation using pyridylideneamides (PYAs)<sup>11</sup> as electronically flexible and adaptive ligand sites (Figure 1a). Pyridylideneamides share features that have been exploited also in the chemistry of N-heterocyclic carbenes (NHCs),<sup>12</sup> in particular the accessibility of a neutral and a mesoionic resonance structure,<sup>13</sup> and their suitability for metal coordination. In contrast to NHCs such as imidazolylidenes and triazolylidenes

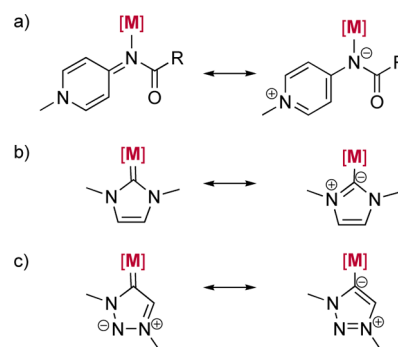


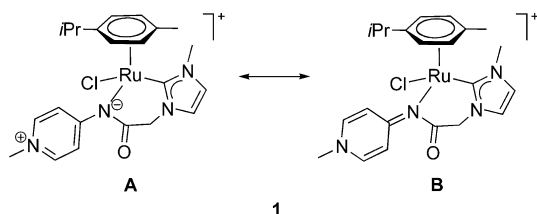
**Figure 1.** Generic representation of limiting resonance structures of (a) PYA, (b) normal NHC, and (c) abnormal NHC metal complexes featuring a formally neutral or anionic donor site.

Received: June 18, 2015

(Figure 1b,c), which have been extensively studied as ligands to transition metal complexes for catalysis<sup>14</sup> and other applications,<sup>15,16</sup> PYAs are relatively unexplored as ligands for transition metal complexes.<sup>17</sup> PYAs bind to the metal via the deprotonated amide nitrogen as a potentially neutral or anionic donor site.<sup>18</sup> The  $\sigma$ -electron-donating properties of PYAs as ligands have been addressed using IR spectroscopy, and they exhibit similar  $\sigma$ -electron donation toward metal centers as normal imidazolylidenes.<sup>19</sup>

We have recently prepared ruthenium complex **1** bearing a chelating ligand composed of both a PYA and NHC donor site (Scheme 1).<sup>20</sup> Even though the complex assumes a solvent-

**Scheme 1. Limiting Resonance Structures of the PYA Wingtip A and B of the Previously Reported Ruthenium Complex 1**



dependent electron distribution in solution, the catalytic activity in hydrogen transfer reactions was only weak. The available data suggest that stronger donation of the ligand to the ruthenium center enhances catalytic activity, although complex degradation was demonstrated to occur readily under the basic conditions used for catalysis, involving in particular the highly base-labile CH<sub>2</sub> group interlinking the imidazole heterocycle and the amide group.<sup>21</sup> Intrigued by these initial results, we surmised that using a 1,2,3-triazolylidene<sup>22</sup> as NHC anchor for the PYA ligand would avoid the drawbacks of the initial ligand design. Specifically, the presence of a carbon adjacent to the carbenic donor site allows the PYA to be connected directly to the carbene, a linkage that is not accessible in Arduengo-type imidazolylidenes due to the lability of the carbonyl group in the imidazolium precursor, yet readily available in triazolium salts via versatile copper-catalyzed azide-alkyne cycloaddition (CuAAC).<sup>23</sup> Moreover, the stronger donor properties of the triazolylidenes when compared to imidazolylidenes<sup>22,24</sup> and the enhanced mesoionic character of the abnormal carbene<sup>25</sup> should further expedite the catalytic activity. Here we demonstrate that PYA-functionalized triazolylidene ligands are highly flexible when coordinated to a ruthenium(II) center and that the electron density at the metal center is substantially altered depending on the solvent-imparted prevailing resonance

structure of the PYA ligand. This efficiency of the ligand to adapt to the environment is remarkable and provides a new strategy for optimizing catalytic reactions, as demonstrated here in ketone transfer hydrogenation.

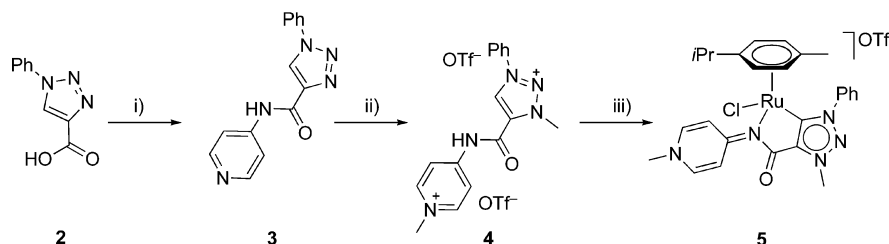
## RESULTS

**Synthesis.** The PYA triazolylidene complex was prepared following the procedure in Scheme 2. The carboxylic acid triazole **2**, prepared via a previously reported procedure,<sup>26</sup> was refluxed in thionyl chloride for 18 h to afford the acyl chloride-functionalized triazole. The reaction was monitored by <sup>1</sup>H NMR spectroscopy in DMSO-*d*<sub>6</sub>, and the disappearance of the carboxylic acid proton signal at 13.00 ppm indicated conversion to the acyl halide. The acyl halide was reacted in situ with 4-aminopyridine in the presence of NiPr<sub>2</sub>Et to yield the pyridylamide-substituted triazole **3**. Formation of **3** was indicated by the low-field singlet resonance at 11.00 ppm corresponding to the amide NH. In addition, the pyridine protons *ortho* to the amide are significantly shielded (doublet at  $\delta = 7.90$ ) as compared to the protons *ortho* to the pyridinic nitrogen (multiplet at  $\delta_{\text{H}} = 8.54$ – $8.45$ ).

Alkylation of **3** with excess methyl triflate proceeded simultaneously at the triazole and pyridine nitrogens. The decreased nucleophilic character of the amide nitrogen prevents methylation in this position under the conditions used. In addition to the appearance of two signals at  $\delta_{\text{H}} = 4.73$  and  $4.32$  for the N-bound methyl groups, the triazolium proton resonance in **4** is diagnostically deshielded at  $\delta_{\text{H}} = 9.79$  (cf.  $\delta_{\text{H}} = 9.51$  in the triazole **3**). The pyridinium protons also shift downfield in the spectrum to 8.80 and 8.33 ppm, thus indicating pyridine methylation.

Ruthenation of **4**, and formation of complex **5**, was achieved via formation of a Ag–NHC intermediate and in situ carbene transfer to [Ru(*p*-cym)Cl<sub>2</sub>]<sub>2</sub> in the presence of Me<sub>4</sub>NCl. The chloride salt serves both as a means of removing silver upon transmetalation and to prevent scrambling of the anionic ancillary ligand in the ruthenium complex (Cl<sup>−</sup> vs OTf<sup>−</sup>). The excess Ag<sub>2</sub>O used for the first step of this metalation presumably deprotonates the amide nitrogen, in addition to forming the silver–NHC complex, as the acidic character of the amide proton is significantly higher than that of the triazolium salt.<sup>27</sup> Triazolylidene coordination to the ruthenium center was indicated by the absence of the low-field proton resonance and the carbene carbon resonance in the <sup>13</sup>C NMR spectrum at  $\delta_{\text{C}} = 165.3$ , in agreement with previously reported triazolylidene ruthenium complexes.<sup>28</sup> The absence of an amide proton in the <sup>1</sup>H NMR spectrum as well as the splitting of the aromatic *p*-cymene protons into four distinct doublets suggests chelation and hence *N*,*C*-bidentate coordination of the PYA triazolyl-

**Scheme 2. Synthesis of the Ruthenium Complex 5, Bearing the Mixed PYA Triazolylidene Ligand<sup>a</sup>**



<sup>a</sup>Reagents and conditions: (i) first SOCl<sub>2</sub>,  $\Delta T$ , then 4-aminopyridine, NiPr<sub>2</sub>Et, CH<sub>2</sub>Cl<sub>2</sub>; (ii) MeOTf, CH<sub>2</sub>Cl<sub>2</sub>; (iii) Ag<sub>2</sub>O, [Ru(*p*-cym)Cl<sub>2</sub>]<sub>2</sub>, Me<sub>4</sub>NCl, MeCN.

dene ligand in complex **5**. The carbonyl carbon of the amide group is shifted downfield from 155.6 ppm in **4** to 171.0 ppm in **5** as a consequence of amide coordination to the ruthenium center.

The formation of **5** was unambiguously confirmed by single-crystal X-ray diffraction analysis. Suitable crystals of this complex were obtained by diffusion of Et<sub>2</sub>O into a CH<sub>2</sub>Cl<sub>2</sub> solution of **5**. The molecular structure features the classical three-legged piano-stool geometry with the ruthenium center in a pseudotetrahedral geometry (Figure 2). The Ru–C1 bond

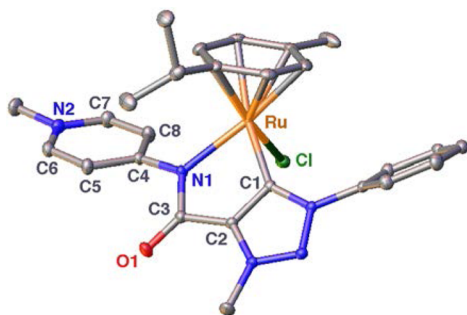


**Figure 2.** ORTEP presentation of complex **5** (50% probability; hydrogen atoms, cocrystallized H<sub>2</sub>O molecule, and the noncoordinated OTf<sup>−</sup> anion omitted for clarity). Selected bond lengths and angles: Ru–C1 2.0119(11) Å, C4–C5 1.4057(16) Å, C4–C8 1.4046(18) Å, C5–C6 1.3756(17) Å, C7–C8 1.3669(18) Å; C1–Ru–N1 76.18(4)°.

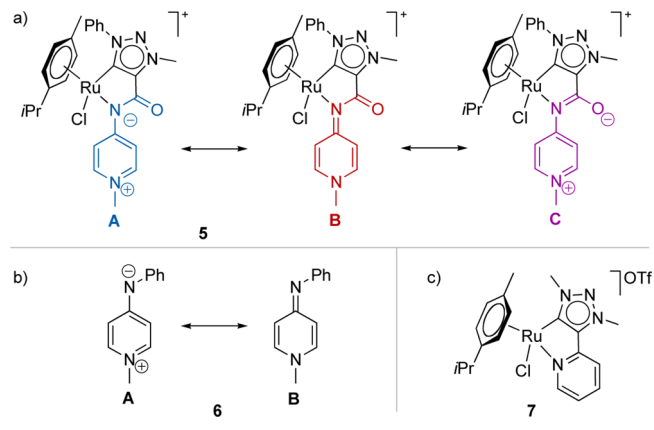
length is 2.012(1) Å, which is typical for this type of carbene ruthenium complexes.<sup>28,29</sup> In the pyridyl heterocycle, the C4–C5 (1.406(2) Å) and C4–C8 bonds (1.405(2) Å) are significantly longer than the bonds linking C6–C5 (1.376(2) Å) and C7–C8 (1.367(2) Å), similar to the corresponding bond lengths in related PYA imidazolylidene complexes.<sup>20</sup> This partial double-bond localization indicates a predominance of the neutral resonance structure (cf. Figure 1a left) in the solid state with less contribution from a delocalized aromatic system comprising a mesoionic ground state (cf. Figure 1a, right). However, the C4–N1 bond length is not particularly short, 1.390(2) Å, indicating only little double-bond character.

Complex **5** is considerably more stable than the analogous complex **1**, containing a benzylic CH<sub>2</sub> linker between the NHC donor and the PYA system. Thus, a methanolic solution of complex **5** is stable over several weeks in the presence of 5 equiv of KOH, even when kept at elevated temperatures (reflux). Likewise, complex **5** is not altered when exposed to aqueous HCl (D<sub>2</sub>O solution) at room temperature. However, heating this acidic solution to 80 °C led to gradual decomposition.

**Resonance Structure Dynamics.** UV–vis and NMR spectroscopic techniques as well as electrochemical analyses were used to assess the electronic flexibility of the PYA ligand when confined at the ruthenium center through chelation. Specifically, the contributions of different resonance structures (A, B, C, Scheme 3a) with various degrees of mesoionic character and variable donor ability of the N-donor ligand were probed by modifying the polarity of the environment.

Previous studies on complex **1** and on the parent pyridylideneamine **6** (Scheme 3b) indicated that the NMR chemical shift difference between the pyridinic  $\alpha$  and  $\beta$  protons constitutes a diagnostic probe for the prevalence of the neutral or mesoionic resonance structure.<sup>20,30</sup> Accordingly, an

**Scheme 3.** (a) Limiting Resonance Structures A, B, and C of the PYA Wingtip of Complex **5**; (b) Limiting Resonance Structures in the Parent Pyridylideneamine **6**; (c) Complex **7** Containing an Identical Donor Set to Complex **5** but Lacking a Resonance Structure Ambiguity



increased downfield shift of H <sub>$\alpha$</sub>  and concomitant shielding of H <sub>$\beta$</sub>  indicate a higher contribution of the enamine resonance form B (Scheme 3). Thus, analysis of the shift difference in various solvents provides insights into the flexibility of the electron density distribution in complex **5**. The assignment of H <sub>$\alpha$</sub>  and H <sub>$\beta$</sub>  in the NMR spectra was unambiguously confirmed by a nuclear Overhauser effect (NOE), which was exclusively observed between the pyridinium-bound methyl group ( $\delta_{\text{H}} \approx 4.2$ ) and the pyridyl H <sub>$\alpha$</sub>  doublet. Representative spectra in CD<sub>2</sub>Cl<sub>2</sub>, CD<sub>3</sub>OD, and DMSO-*d*<sub>6</sub> indicate a progressive shift of the two resonances in opposite direction (Figure 3), thus supporting a larger contribution of the mesoionic resonance form A in more polar solvents. The sum of the shift difference of H <sub>$\alpha$</sub>  to higher field and of H <sub>$\beta$</sub>  to lower field, i.e.,  $\Delta\delta = \Delta\delta(\text{H}_{\alpha}) - \Delta\delta(\text{H}_{\beta})$ , suggests a correlation with the solvent polarity.<sup>31</sup> Taking the spectrum in CD<sub>2</sub>Cl<sub>2</sub> as a reference ( $\epsilon_{\text{CD}_2\text{Cl}_2} = 9.08$ ; two doublets at  $\delta_{\text{H}} = 8.58$  and 8.17) the signals shift by  $\Delta\delta = 0.33$  in CD<sub>3</sub>OD ( $\epsilon_{\text{MeOH}} = 32.6$ ) and even further by  $\Delta\delta = 0.53$  in DMSO-*d*<sub>6</sub> ( $\epsilon_{\text{DMSO}} = 46.7$ ).<sup>32</sup> This correlation between chemical shift difference and solvent polarity is remarkably linear. A similar solvent-dependent shift was observed for the aromatic proton resonances of the cymene ligand, in agreement with a variable electron density at ruthenium when changing solvents. We have not attempted to numerically evaluate the change of resonance frequencies due to the more complex pattern of the signals. However, it is worth noting that the reference complex **7** with triazolylidene pyridine chelate—which does not have an easily accessible mesoionic resonance structure—does not show a similar solvent-induced change of the resonance frequencies (Figure S2). While a minor shift of all frequencies is observed upon changing the solvents, the relative positions are only marginally affected, thus underpinning more significant changes in complex **5**.

Comparison of the overall chemical shift differences suggests a substantially more pronounced resonance change in complex **5** than in complex **1** ( $\Delta\delta = 0.33$  in **5** vs 0.14 ppm in **1** for a change between CD<sub>2</sub>Cl<sub>2</sub> and CD<sub>3</sub>OD). Accordingly, the ligand in complex **5** reveals a higher adaptability of the ligand, similar to the parent pyridylideneamine **6** ( $\Delta\delta = 0.61$  for CD<sub>2</sub>Cl<sub>2</sub> vs DMSO, cf.  $\Delta\delta = 0.53$  for **5**). These data thus imply that complex **5** comprises a mesoionic N-donor ligand in polar media, while the neutral resonance structure is more relevant in

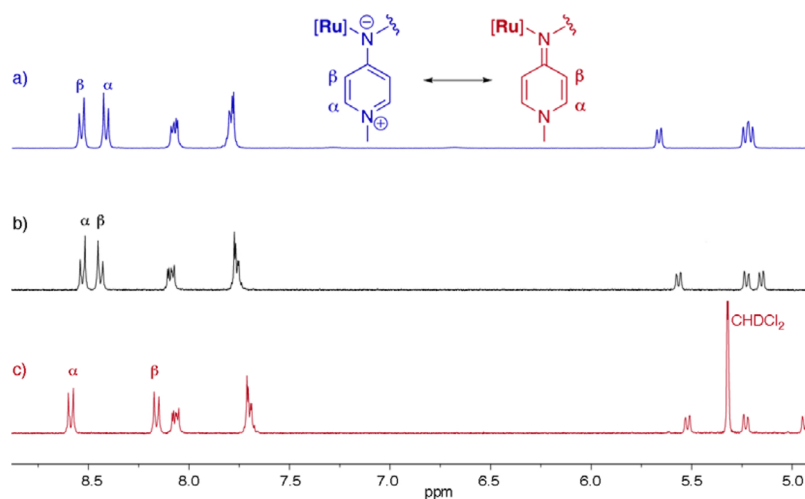


**Figure 3.** Section of the  $^1\text{H}$  NMR spectrum of complex **5** in (a)  $\text{DMSO}-d_6$ , (b)  $\text{CD}_3\text{OD}$ , and (c)  $\text{CD}_2\text{Cl}_2$ , indicating the diagnostic shift of the  $\alpha$  and  $\beta$  protons of the N-mesoionic ligand.

apolar media. This donor flexibility of the PYA ligand in **5** with a coplanar triazolylidene chelate is considerably more pronounced than in complex **1**, with an  $\text{sp}^3$ -hybridized carbon linking the PYA and the N-heterocyclic carbene.

Further support for the adaptability of the complex was obtained by UV–vis spectroscopy. Spectral data of complex **5** and the ligand precursor **4** were measured in MeOH and  $\text{CH}_2\text{Cl}_2$ . In MeOH, the UV–vis spectrum of **5** displays two absorption maxima at 312 and 389 nm, whereas in  $\text{CH}_2\text{Cl}_2$  these maxima are shifted bathochromic to 321 and 401 nm (Figure 4). The higher energy absorption (312 nm in MeOH

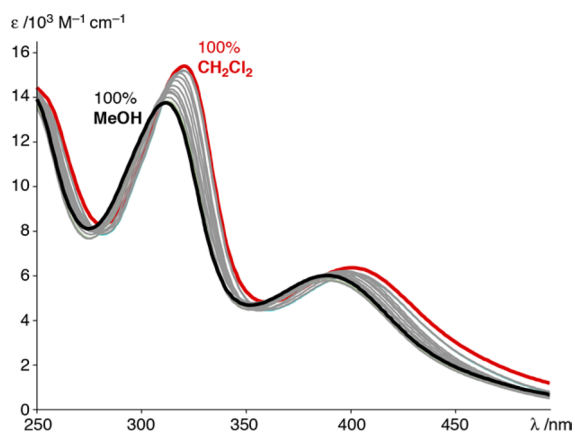


**Figure 4.** Overlaid UV–vis spectra of **5** in varying degrees of  $\text{CH}_2\text{Cl}_2$  and MeOH.

and 321 nm in  $\text{CH}_2\text{Cl}_2$ ) are in the range expected for intraligand charge transfer bands ( $\pi$ – $\pi^*$  transitions). Thus, the lower energy of the maximum absorbed radiation in  $\text{CH}_2\text{Cl}_2$  indicates a variation in the conjugation of the ligand  $\pi$ -system. The quinoid-type resonance structure of **5B** has a higher degree of conjugation than that of the pyridinium resonance structure **5A** (cf. Scheme 3a). The longer wavelength absorbances (389 and 401 nm) are indicative of metal–ligand charge transfer bands (LMCT or MLCT). The wavelength of absorbed radiation increases when the experiment is carried out in  $\text{CH}_2\text{Cl}_2$  (from 389 to 401 nm); therefore the charge transfer energy is lowered in nonpolar media. Resonance structure **B** prevails in nonpolar media, thus lowering the ligand-centered

LUMO as compared to **A** (i.e., increased  $\pi$ -acidity of the ligand). According to such a rationale, the increase of  $\lambda_{\text{max}}$  when moving from MeOH to  $\text{CH}_2\text{Cl}_2$  suggests that the high-energy absorption is an MLCT and not a LMCT band. When the polarity of the solution of **5** was decreased incrementally (Figure 4 and Table S1), the wavelengths of the absorption maxima gradually shift to longer wavelength, thus inferring that the prevalence of one limiting resonance structure over the other is easily controlled by adjustment of the polarity of the solution.

Likewise, the ligand precursor **4** absorbs at higher wavelength when dissolved in  $\text{CH}_2\text{Cl}_2$  ( $\lambda_{\text{max}} = 285$  and 345 nm) as compared to MeOH ( $\lambda_{\text{max}} = 280$  and 341 nm, Figure S1). This behavior is similar to that of the complex and indicates that different resonance structures may be preponderant also for the protonated ligand precursor as well; however, the changes are less pronounced and the intraligand charge transfer bands shift by only 4 nm, while the  $\Delta\lambda_{\text{max}}$  in complex **5** increases to 9 nm.

These results corroborate the trend deduced from NMR spectroscopy and further suggest that altering the dielectric constant of the solvent increases the prevalence of one limiting resonance structure over another. In more polar solvents the mesoionic pyridinium-amidate resonance structure is more relevant, whereas in less polar solvents the neutral quinoid-type imine resonance structure prevails.

Resonance structure **C**, with an oxygen-centered anionic charge, is less prevalent according to IR spectroscopy. Complex **5** displayed absorptions at  $1656\text{ cm}^{-1}$  in  $\text{CH}_2\text{Cl}_2$  and  $1653\text{ cm}^{-1}$  in MeOH for the stretching frequency of the amide  $\text{C}=\text{O}$  bond in the infrared spectrum. The similarity of the absorptions indicates that the amide  $\text{CO}$  is not altered upon dissolution in more polar solvents. Previous DFT studies predict that the metal–nitrogen bond is highly polarized and therefore disfavors charge migration to a remote carbonyl site.<sup>19</sup>

Electrochemical analyses provided further evidence for the electronic adaptability of the PYA ligand. Cyclic voltammetry (CV) experiments in  $\text{CH}_2\text{Cl}_2$  revealed a reversible and presumably ruthenium-centered oxidation at  $E_{1/2} = +1.20\text{ V}$  vs SCE for **5** (Figure 5) and an irreversible, potentially catalytic reduction with a maximum at  $E_{\text{pc}} = -1.25\text{ V}$ . However, when the measurement was performed in  $\text{MeNO}_2$  ( $\epsilon = 35.87$ ), the oxidation potential was significantly lower, at  $E_{1/2} = +1.11\text{ V}$ . This 90 mV potential difference suggests a solvent-induced

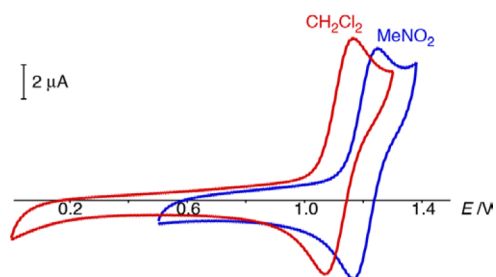
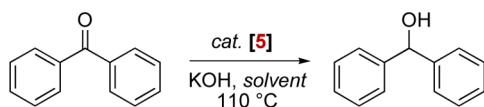


**Figure 5.** Superimposed CV plots of complex **5** in  $\text{CH}_2\text{Cl}_2$  and  $\text{MeNO}_2$ , indicating the solvent-induced 90 mV shift of oxidation potential.

change of the electron density at the metal center.<sup>33</sup> Easier oxidation of the ruthenium center in  $\text{MeNO}_2$  may be imparted by the stronger ligand donation in this solvent, likely owing to the mesoionic resonance form **A** (cf. *Scheme 3a*). The neutral resonance form **B** features a neutral  $\pi$ -acidic imine donor rather than an anionic amide  $\text{NR}_2^-$ , and this form would be expected to be more relevant in less polar  $\text{CH}_2\text{Cl}_2$ . This conclusion is in agreement with the complementary data acquired by UV–vis and NMR spectroscopic analyses and further underlines the strong solvent-dependent donor flexibility of the PYA triazolylidene ligand. The donor properties of this ligand can be tuned readily through solvent-polarity-induced prevalence of either the limiting resonance structure **A** or **B**.<sup>30,34</sup>

**Catalytic Applications.** The catalytic activity of complex **5** in the hydrogen transfer reactions was evaluated by using benzophenone to diphenylmethanol hydrogenation.<sup>35</sup> Under standard transfer hydrogenation conditions using *i*PrOH as dihydrogen source and solvent, complex **5** displayed good catalytic activity and reached 92% conversion of the starting material to the alcohol after 24 h (*Table 1*, entry 1; see also

**Table 1.** Catalytic Transfer Hydrogenation and Reduction of Benzophenone in *i*PrOH<sup>a</sup>



entry	solvent system <sup>b</sup>	yield (%) 2 h/24 h
1	<i>i</i> PrOH	19/92
2	<i>i</i> PrOH/DMA (9:1)	24/99
3	<i>i</i> PrOH/DMA (8:2)	23/98
4	<i>i</i> PrOH/DMA (7:3)	11/88
5	<i>i</i> PrOH/DMA (6:4)	10/44
6	<i>i</i> PrOH/DMA (1:1)	0/0

<sup>a</sup>General reaction conditions: benzophenone (1 mmol), anisole (0.2 mmol, internal standard), catalyst (0.01 mmol), KOH (50  $\mu\text{L}$  of 2 M aqueous solution, 10 mol %), refluxed at 110  $^\circ\text{C}$ . <sup>b</sup>Solvent mixtures in v/v, total volume 5.0 mL.

*Figure S3*). This result is a significant improvement when compared to previously reported complexes containing PYA imidazolylidene ligands,<sup>20</sup> probably due to the enhanced stability of the complex toward basic degradation. Indeed, no precipitate was observed at later stages of the reaction that might indicate decomposition of the complex, and in fact it was possible to recover complex **5** after catalytic runs, as confirmed by NMR spectroscopy. The enhanced stability is likely a direct consequence of the ligand design, specifically the absence of an

acidic  $\text{CH}_2$  group between the pyridylamide group and the heterocyclic carbene.

Interestingly, increasing the polarity of the reaction medium from pure *i*PrOH ( $\epsilon = 17.9$ ) by addition of dimethylacetamide (DMA,  $\epsilon = 37.8$ ) as cosolvent had a notable impact on the catalytic activity (entries 2, 3). Under these conditions, complex **5** achieves essentially full conversion after 24 h and 24% conversion after 2 h (cf. 19% in pure *i*PrOH). This higher activity was attributed to and increased relevance of resonance structure **A** over **B** (cf. *Scheme 3b*) upon increasing the permittivity, which presumably increases the donor strength of the PYA NHC ligand, as deduced from spectroscopy and electrochemistry (see above). Modification of the solvent ratio revealed an optimum performance at an *i*PrOH/DMA mixture ratio of 9:1 and 8:2 v/v, while the addition of larger proportions of DMA decreased the catalytic activity (entries 4–6). At a 1:1 (v/v) *i*PrOH/DMA solvent ratio, the catalytic activity is lost completely. These results suggest that the catalytic activity is not exclusively governed by the solvent dielectric constant but by a combination of factors, as both complex solubility and sufficient availability of the  $\text{H}_2$ -donor source will impact catalytic activity.<sup>36</sup>

In order to evaluate the specific role of the PYA ligand and the relevance of mesoionic ligands, the pyridyl-substituted triazolylidene ruthenium complex **7** (*Figure 6*) was subjected to

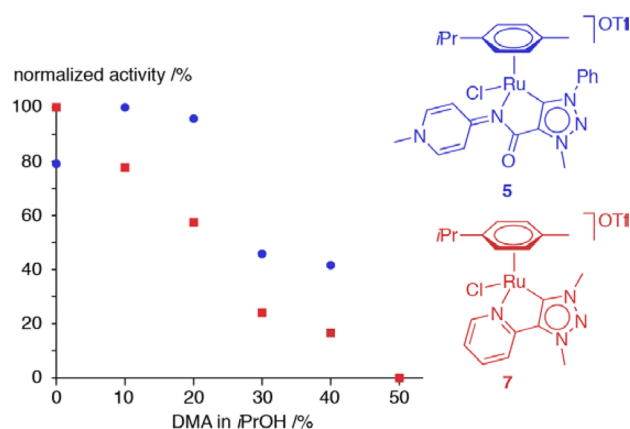


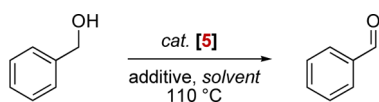
**Figure 6.** Dependence of catalytic activity on the solvent media for complex **5** with an adaptive PYA ligand and for complex **7** with a static pyridyl donor (activity after 120 min for **5**, after 8 min for **7**, normalized to highest performance).

similar transfer hydrogenation catalysis.<sup>37</sup> With this complex, a swap between mesoionic and neutral resonance forms of the N-donor ligand is suppressed. Under standard transfer hydrogenation conditions using *i*PrOH as dihydrogen source and solvent, complex **7** displayed almost quantitative yields after 20 min (*Figure S4*). However, increasing the polarity of the reaction medium by addition of DMA did not follow the same reactivity profile as shown by complex **5**, and the catalytic activity continuously and substantially decreased and reached the same 0% conversion in a 1:1 *i*PrOH/DMA solvent ratio (*Figures 6* and *S4*). This divergence of complex **7** to the behavior of complex **5** is significant and indicates that DMA has only an inhibitive effect for complex **7**, but has an accelerating effect for complex **5**, at least when employed in small proportion. This contrasting response to solvent mixtures suggests that, indeed, the mesoionic properties of PYA-type

ligands can be exploited to promote bond activation and catalytic activity.<sup>38</sup>

Stimulated by precedent activity of related ruthenium triazolylidene complexes,<sup>39</sup> the activity of **5** was evaluated as a catalyst precursor for base- and oxidant-free alcohol oxidation in addition to transfer hydrogenation. When using benzyl alcohol as a model substrate, the activity of complex **5** in this process was much lower than the performance observed in transfer hydrogenation of benzophenone (Table 2). However, a

**Table 2. Catalytic Dehydrogenation of Benzyl Alcohol to Benzaldehyde<sup>a</sup>**



entry	solvent	additive	yield (%) 4 h/24 h
1	toluene		nd/10
2	1,2-DCB		nd/9
3	DMA		nd/22
4	DMA	Cs <sub>2</sub> CO <sub>3</sub>	30/30
5	DMA	K <sub>2</sub> CO <sub>3</sub>	72/72
6	DMA	KOH	16/30
7	DMA	AgOTf	52/67
8	DMA	MeOTf	12/22
9	DMA	NiPr <sub>2</sub> Et	14/34

<sup>a</sup>General reaction conditions: benzyl alcohol (0.2 mmol), catalyst (0.01 mmol), additive (0.02 mmol), and solvent (2.0 mL) were heated to 110 °C; 1,2-DCB = 1,2-C<sub>6</sub>H<sub>4</sub>Cl<sub>2</sub>, OTf = CF<sub>3</sub>SO<sub>3</sub>, nd = not determined.

similar dependence of the conversion on solvent permittivity was apparent: in toluene ( $\epsilon = 2.38$ ) and 1,2-dichlorobenzene ( $\epsilon = 9.93$ ), the reaction reached just 10% conversion at 24 h, while in DMA up to 20% conversion were achieved within the same time (entries 1–3). While previous work has shown that chelating triazolylidenes are less powerful catalysts for this dehydrogenation reaction,<sup>37</sup> these conversions were still substantially lower than expected, in particular when considering that the complex is an effective catalyst precursor for *i*PrOH oxidation as a side reaction in the base-free transfer hydrogenation (see above). In an attempt to enhance the catalytic activity, a variety of additives were evaluated for catalyst activation, in particular for potential halide abstraction as an initial step to facilitate alcohol coordination to the ruthenium center (entries 4–9). Significant improvement of catalytic activity was accomplished when using K<sub>2</sub>CO<sub>3</sub> or AgOTf (yields around 70%, entries 5, 7), and milder bases such as NiPr<sub>2</sub>Et had no effect (entry 9). Likewise, chloride abstraction with a CH<sub>3</sub><sup>+</sup> source (MeOTf, entry 8) was unsuccessful<sup>40</sup> and led to similar performance to that in the absence of any additive (entry 3).

## CONCLUSIONS

The mixed PYA triazolylidene chelate system introduced here offers various attractive features for further development. The triazolylidene unit provides a reliable anchor for chelation and hence for persistent coordination of the pyridylideneamide ligand. Moreover, the specific positioning of the heteroatoms in 1,2,3-triazolylidenes allows for the introduction of a carbonyl group adjacent to the carbenic donor, an arrangement that is not stable in Arduengo-type 2-imidazolylidene ligands. The

PYA ligand is highly adaptive and assumes different resonance structures depending on the direct environment such as in the solid state or in solvents of different polarity, thus revealing N-mesoionic properties. The solvent-dependent resonance structure contributions modify the donor ability of the ligand and the electron density at the metal center, thus providing a new paradigm for tailoring the activity of the metal center. This adaptive behavior of the ligand is advantageous to facilitate redox processes and to promote catalytic activity. Here, this concept is demonstrated by using different solvent compositions to over- or underweight specific resonance contributions and to enhance the catalytic performance of PYA ruthenium complexes. Hence, such PYA-based ligand systems provide a dynamic platform for inducing and exploiting metal flexibility, a concept that complements the ligand noninnocence and ligand cooperativity principles in catalyst design.

## EXPERIMENTAL SECTION

**General Procedures.** Triazole **2** and complex **7** were synthesized according to previously reported procedures.<sup>26,37</sup> The ruthenium complex was synthesized under strict exclusion of light and air using standard Schlenk techniques under an atmosphere of dry nitrogen. Acetonitrile was dried by passage through a solvent purification column. All other reagents were used as received unless otherwise stated. NMR spectra were recorded on Varian spectrometers operating at 400 or 500 MHz unless otherwise stated. Chemical shifts ( $\delta$  in ppm,  $J$  in Hz) were referenced to SiMe<sub>4</sub>. Signal assignments are based on homo- and heteronuclear (multiple-bond) correlation spectroscopy. Elemental analysis was performed on an Exeter Analytical CE440 elemental analyzer, by the Microanalytical Laboratory at the University College Dublin, Ireland. High-resolution mass spectrometry was carried out with a Micromass/Waters Corp. USA liquid chromatography time-of-flight spectrometer equipped with an electrospray source.

**Electrochemistry.** Electrochemical measurements were carried out using an EG&G Princeton Applied Research potentiostat model 273A typically at a 100 mV s<sup>-1</sup> sweep rate employing a gastight three-electrode cell under an argon atmosphere. A Pt disk with a 3.80 mm<sup>2</sup> surface area was used as the working electrode and was polished before each measurement. The reference electrode was a Ag/AgCl electrode; the counter electrode was a Pt wire. Bu<sub>4</sub>NPF<sub>6</sub> (0.1 M) in dry CH<sub>2</sub>Cl<sub>2</sub> or nitromethane was used as a base electrolyte with analyte concentrations of approximately 10<sup>-3</sup> M. The ferrocenium/ferrocene redox couple was used as an internal reference ( $E_{1/2} = +0.46$  V and +0.35 V vs SCE in CH<sub>2</sub>Cl<sub>2</sub> and MeNO<sub>2</sub>, respectively).<sup>41</sup>

**Triazole 3.** Under a N<sub>2</sub> atmosphere, the acid **2** (2.835 g, 15 mmol) was refluxed in SOCl<sub>2</sub> (15 mL) for 3 h. Excess SOCl<sub>2</sub> was removed under reduced pressure in a well-ventilated fumehood. The residue was dissolved in dry CH<sub>2</sub>Cl<sub>2</sub> (60 mL), then DIPEA (3.14 mL, 18 mmol) and 4-aminopyridine (1.41 g, 15 mmol) were added, and the reaction mixture was stirred at room temperature for 18 h. Removal of solvent in vacuo and washing the residue with H<sub>2</sub>O (50 mL) afforded the product triazole as a gray solid (yield 3.718 g, 94%). <sup>1</sup>H NMR (400 MHz, (CD<sub>3</sub>)<sub>2</sub>SO):  $\delta = 11.00$  (s, 1H, NH), 9.51 (s, 1H, CH<sub>trz</sub>), 8.54–8.45 (m, 2H, H<sub>py</sub><sup>ortho N</sup>), 8.01 (d, <sup>3</sup>J<sub>HH</sub> = 7.7 Hz, 2H, H<sub>ph</sub><sup>ortho</sup>), 7.90 (d, <sup>3</sup>J<sub>HH</sub> = 7.9 Hz, 2H, H<sub>py</sub><sup>ortho C</sup>), 7.64 (t, <sup>3</sup>J<sub>HH</sub> = 7.9 Hz, 2H, H<sub>ph</sub><sup>meta</sup>), 7.55 (t, <sup>3</sup>J<sub>HH</sub> = 7.9 Hz, 1H, H<sub>ph</sub><sup>para</sup>). <sup>13</sup>C{<sup>1</sup>H} NMR (101 MHz, (CD<sub>3</sub>)<sub>2</sub>SO):  $\delta = 159.0$  (CO), 150.3 (CH<sub>py</sub><sup>ortho N</sup>), 145.3 (C<sub>py</sub>), 143.2 (C<sub>trz</sub>), 136.2 (C<sub>ph</sub>), 130.0 (CH<sub>ph</sub><sup>ortho</sup>), 129.4 (CH<sub>trz</sub>), 126.2 (CH<sub>ph</sub><sup>para</sup>), 120.6 (CH<sub>ph</sub><sup>meta</sup>), 114.2 (CH<sub>py</sub><sup>ortho C</sup>). HR-MS (ESI<sup>+</sup>)  $m/z = 266.1054$  (calcd for [M + H]<sup>+</sup> 266.1042).

**Pyridinium-triazolium Triflate 4.** The triazole **3** (1.281 g, 4.8 mmol) was suspended in CH<sub>2</sub>Cl<sub>2</sub> (50 mL) and stirred at 0 °C for 10 min. MeOTf (2.64 mL, 24.2 mmol) was added, and the reaction was stirred at 0 °C for 30 min, followed by room-temperature stirring for 18 h. The mixture was filtered, and the filtrate was washed with Et<sub>2</sub>O (100 mL) and pentane (100 mL), to afford the product as an off-white solid (yield 1.890 g, 96%). <sup>1</sup>H NMR (400 MHz, CD<sub>3</sub>OD):  $\delta = 9.79$  (s,

$^1\text{H}$ ,  $H_{\text{trz}}$ ), 8.80 (d,  $^3J_{\text{HH}} = 7.2$  Hz, 2H,  $H_{\text{py}}^{\text{ortho N}}$ ), 8.33 (d,  $^3J_{\text{HH}} = 7.2$  Hz, 2H,  $H_{\text{py}}^{\text{ortho C}}$ ), 8.03–8.01 (m, 2H,  $H_{\text{ph}}^{\text{ortho}}$ ), 7.80–7.76 (m, 3H,  $H_{\text{ph}}^{\text{meta/para}}$ ), 4.73 (s, 3H,  $\text{N}_{\text{trz}}\text{CH}_3$ ), 4.32 (s, 3H,  $\text{N}_{\text{py}}\text{CH}_3$ ), NH not resolved.  $^{13}\text{C}\{^1\text{H}\}$  NMR (101 MHz,  $\text{CD}_3\text{OD}$ ):  $\delta = 155.6$  (CO), 152.5 ( $\text{C}_{\text{py}}$ ), 147.7 ( $\text{CH}_{\text{py}}^{\text{ortho N}}$ ), 136.3 ( $\text{C}_{\text{trz}}$ ), 136.2 ( $\text{C}_{\text{ph}}^{\text{ipso}}$ ), 133.6 ( $\text{CH}_{\text{ph}}^{\text{para}}$ ), 131.8 ( $\text{CH}_{\text{ph}}^{\text{meta}}$ ), 130.7 ( $\text{CH}_{\text{trz}}$ ), 123.0 ( $\text{CH}_{\text{ph}}^{\text{ortho}}$ ), 121.7 (q,  $^1J_{\text{CF}} = 318.6$  Hz,  $\text{SCF}_3$ ), 117.7 ( $\text{CH}_{\text{py}}^{\text{ortho C}}$ ), 47.7 ( $\text{N}_{\text{trz}}\text{CH}_3$ ), 42.1 ( $\text{N}_{\text{py}}\text{CH}_3$ ). HR-MS (ESI<sup>+</sup>):  $m/z = 616.0460$  (calcd for  $[\text{M} + \text{Na}]^+$  616.0371).

**Complex 5.** The salt **4** (208 mg, 0.35 mmol),  $\text{Ag}_2\text{O}$  (81 mg, 0.35 mmol),  $[\text{Ru}(p\text{-cym})\text{Cl}_2]_2$  (107 mg, 0.18 mmol), and  $\text{NMe}_4\text{Cl}$  (115 mg, 1.05 mmol) were suspended in dry MeCN (10 mL) and heated to 60 °C for 18 h. The resulting mixture was filtered through a short pad of Celite, concentrated in vacuo, and precipitated from  $\text{Et}_2\text{O}$  (50 mL). The resulting solid was dissolved in the minimum amount of  $\text{CH}_2\text{Cl}_2$  (ca. 2 mL) and filtered through Celite. The solution was concentrated to 1 mL, and addition of  $\text{Et}_2\text{O}$  (50 mL) afforded the product as a spectroscopically pure yellow solid (yield 209 mg, 84%). An analytically pure sample was obtained upon recrystallization from a  $\text{CHCl}_3$  solution that was layered with  $\text{Et}_2\text{O}$ .  $^1\text{H}$  NMR (500 MHz,  $\text{CD}_2\text{Cl}_2$ ):  $\delta = 8.58$  (d,  $^3J_{\text{HH}} = 7.2$  Hz, 2H,  $H_{\text{py}}^{\text{ortho C}}$ ), 8.17 (d,  $^3J_{\text{HH}} = 7.2$  Hz, 2H,  $H_{\text{py}}^{\text{ortho N}}$ ), 8.08–8.06 (m, 2H,  $H_{\text{ph}}$ ), 7.71–7.67 (m, 3H,  $H_{\text{ph}}$ ), 5.52 (d,  $^3J_{\text{HH}} = 5.9$  Hz, 1H,  $H_{\text{cym}}$ ), 5.23 (d,  $^3J_{\text{HH}} = 5.9$  Hz, 1H,  $H_{\text{cym}}$ ), 4.94 (d,  $^3J_{\text{HH}} = 5.8$  Hz, 1H,  $H_{\text{cym}}$ ), 4.47 (d,  $^3J_{\text{HH}} = 5.8$  Hz, 1H,  $H_{\text{cym}}$ ), 4.43 (s, 3H,  $\text{N}_{\text{trz}}\text{CH}_3$ ), 4.19 (s, 3H,  $\text{N}_{\text{pyr}}\text{CH}_3$ ), 2.20 (septet,  $^3J_{\text{HH}} = 6.9$  Hz, 1H,  $H_{\text{cym}}$ ), 2.12 (s, 3H,  $\text{CH}_3\text{-cym}$ ), 0.94 (d,  $^3J_{\text{HH}} = 6.9$  Hz, 3H,  $\text{CH}_3\text{-cym}$ ), 0.91 (d,  $^3J_{\text{HH}} = 6.9$  Hz, 3H,  $\text{CH}_3\text{-cym}$ ).  $^{13}\text{C}\{^1\text{H}\}$  NMR (101 MHz,  $\text{CD}_2\text{Cl}_2$ ):  $\delta = 171.0$  (CO), 167.3 ( $\text{C}_{\text{py}}^{\text{ipso}}$ ), 165.3 ( $\text{C}_{\text{trz}}\text{Ru}$ ), 143.3 ( $\text{C}_{\text{py}}^{\text{ortho N}}$ ), 139.9 ( $\text{C}_{\text{trz}}$ ), 138.5 ( $\text{C}_{\text{ph}}^{\text{ipso}}$ ), 131.5 ( $\text{C}_{\text{ph}}$ ), 130.3 ( $\text{C}_{\text{ph}}$ ), 125.3 ( $\text{C}_{\text{ph}}$ ), 123.5 ( $\text{C}_{\text{py}}^{\text{ortho C}}$ ), 103.9 ( $\text{C}_{\text{cym-Ph}}$ ), 102.9 ( $\text{C}_{\text{cym-Ph}}$ ), 93.3 ( $\text{CH}_{\text{cym-Ph}}$ ), 88.1 ( $\text{CH}_{\text{cym-Ph}}$ ), 83.6 ( $\text{CH}_{\text{cym-Ph}}$ ), 81.2 ( $\text{CH}_{\text{cym-Ph}}$ ), 46.9 ( $\text{N}_{\text{pyr}}\text{CH}_3$ ), 37.2 ( $\text{N}_{\text{trz}}\text{CH}_3$ ), 31.6 ( $\text{CH}_{\text{cym}}$ ), 22.5 ( $\text{CH}_3\text{-cym}$ ), 22.2 ( $\text{CH}_3\text{-cym}$ ), 18.7 ( $\text{CH}_3\text{-cym}$ ),  $\text{SCF}_3$  not resolved. HR-MS (ESI<sup>+</sup>):  $m/z = 564.1118$  (calcd for  $[\text{M} - \text{OTf}]^+$  564.1104). IR ( $\text{CH}_2\text{Cl}_2$ ):  $\nu_{\text{CO}} = 1656$   $\text{cm}^{-1}$ . Anal. Calcd for  $\text{C}_{27}\text{H}_{29}\text{ClF}_3\text{N}_5\text{O}_4\text{RuS}$  (713.13)·0.5 $\text{CHCl}_3$ : C, 42.74; H, 3.85; N, 9.06. Found: C, 42.70; H, 3.91; N, 9.04.

$^1\text{H}$  NMR (400 MHz,  $\text{CD}_3\text{OD}$ ):  $\delta = 8.52$  (d,  $^3J_{\text{HH}} = 7.3$  Hz, 2H,  $H_{\text{py}}^{\text{ortho C}}$ ), 8.44 (d,  $^3J_{\text{HH}} = 7.3$  Hz, 2H,  $H_{\text{py}}^{\text{ortho N}}$ ), 8.10–8.07 (m, 2H,  $H_{\text{ph}}$ ), 7.77–7.74 (m, 3H,  $H_{\text{ph}}$ ), 5.55 (d,  $^3J_{\text{HH}} = 6.1$  Hz, 1H,  $H_{\text{cym}}$ ), 5.21 (d,  $^3J_{\text{HH}} = 6.1$  Hz, 1H,  $H_{\text{cym}}$ ), 5.13 (d,  $^3J_{\text{HH}} = 5.7$  Hz, 1H,  $H_{\text{cym}}$ ), 4.58 (d,  $^3J_{\text{HH}} = 5.7$  Hz, 1H,  $H_{\text{cym}}$ ), 4.46 (s, 3H,  $\text{N}_{\text{trz}}\text{CH}_3$ ), 4.20 (s, 3H,  $\text{N}_{\text{pyr}}\text{CH}_3$ ), 2.20 (septet,  $^3J_{\text{HH}} = 6.9$  Hz, 1H,  $H_{\text{cym}}$ ), 2.09 (s, 3H,  $\text{CH}_3\text{-cym}$ ), 0.95 (d,  $^3J_{\text{HH}} = 6.9$  Hz, 3H,  $\text{CH}_3\text{-cym}$ ), 0.94 (d,  $^3J_{\text{HH}} = 6.9$  Hz, 3H,  $\text{CH}_3\text{-cym}$ ).  $^{13}\text{C}\{^1\text{H}\}$  NMR (101 MHz,  $\text{CD}_3\text{OD}$ ):  $\delta = 171.3$  (CO), 168.0 ( $\text{C}_{\text{py}}^{\text{ipso}}$ ), 166.4 ( $\text{C}_{\text{trz}}\text{Ru}$ ), 144.8 ( $\text{C}_{\text{py}}^{\text{ortho N}}$ ), 140.8 ( $\text{C}_{\text{trz}}$ ), 139.6 ( $\text{C}_{\text{ph}}^{\text{ipso}}$ ), 132.3 ( $\text{C}_{\text{ph}}$ ), 131.0 ( $\text{C}_{\text{ph}}$ ), 126.4 ( $\text{C}_{\text{ph}}$ ), 124.3 ( $\text{C}_{\text{py}}^{\text{ortho C}}$ ), 103.8 ( $\text{C}_{\text{cym-Ph}}$ ), 103.7 ( $\text{C}_{\text{cym-Ph}}$ ), 93.9 ( $\text{CH}_{\text{cym-Ph}}$ ), 89.0 ( $\text{CH}_{\text{cym-Ph}}$ ), 84.6 ( $\text{CH}_{\text{cym-Ph}}$ ), 82.7 ( $\text{CH}_{\text{cym-Ph}}$ ), 46.6 ( $\text{N}_{\text{pyr}}\text{CH}_3$ ), 37.3 ( $\text{N}_{\text{trz}}\text{CH}_3$ ), 32.5 ( $\text{CH}_{\text{cym}}$ ), 22.6 ( $\text{CH}_3\text{-cym}$ ), 22.3 ( $\text{CH}_3\text{-cym}$ ), 18.6 ( $\text{CH}_3\text{-cym}$ ),  $\text{SCF}_3$  not resolved. IR (MeOH):  $\nu_{\text{CO}} = 1653$   $\text{cm}^{-1}$ .

**Typical Procedure for the Transfer Hydrogenation of Benzophenone.** Complex **5** (8 mg, 0.01 mmol) was weighed directly into the reaction flask, anisole (20  $\mu\text{L}$ , 0.2 mmol, as internal standard), *i*PrOH (4.5 mL), DMA (0.5 mL), and an aqueous KOH solution (50  $\mu\text{L}$ , 2 M, 0.1 mmol) were added, and the solution was heated at 110 °C for 10 min. The substrate (1.0 mmol) was added. Aliquots (0.1 mL) were taken after fixed times, diluted with  $\text{CD}_3\text{OD}$  (0.6 mL), and analyzed by  $^1\text{H}$  NMR spectroscopy.

**Typical Procedure for the Oxidation of Benzyl Alcohol.** Complex **5** (8 mg, 0.01 mmol), anisole (internal standard, 20  $\mu\text{L}$ , 0.2 mmol), benzyl alcohol (19  $\mu\text{L}$ , 0.2 mmol), and solvent (2 mL) were placed in a vial with a pierced septum and heated to 110 °C. An aliquot (0.1 mL) was taken at fixed times, diluted with  $\text{CDCl}_3$  (0.6 mL), and analyzed by  $^1\text{H}$  NMR spectroscopy.

**Crystallographic Details.** Crystal data for **5** were collected using an Oxford Diffraction (now Rigaku) SuperNova A diffractometer fitted with an Atlas detector and using monochromated Mo  $K\alpha$  radiation (0.710 73 Å). A complete data set was collected, assuming that the Friedel pairs are not equivalent. An analytical numeric absorption correction was performed.<sup>42</sup> The structure was solved by direct

methods using SHELXS-97<sup>43</sup> and refined by full matrix least-squares on  $F^2$  for all data using SHELXL-97.<sup>43</sup> Hydrogen atoms were added at calculated positions and refined using a riding model. Their isotropic thermal displacement parameters were fixed to 1.2 times (1.5 times for methyl groups) the equivalent one of the parent atom. Anisotropic thermal displacement parameters were used for all non-hydrogen atoms. Further crystallographic details are compiled in Table S3. Crystallographic data (excluding structure factors) for **5** have been deposited with the Cambridge Crystallographic Data Centre as supplementary publication no. CCDC 1407377.

## ■ ASSOCIATED CONTENT

### Supporting Information

The Supporting Information is available free of charge on the ACS Publications website at DOI: 10.1021/acs.organo-met.5b00533.

Spectroscopic and electrochemical details and catalytic data for complex **7** (PDF)

Crystallographic data (CIF)

## ■ AUTHOR INFORMATION

### Corresponding Author

\*E-mail: martin.albrecht@dcb.unibe.ch.

### Notes

The authors declare no competing financial interest.

## ■ ACKNOWLEDGMENTS

We thank James Wright for fruitful discussion and the European Research Council (CoG 615653), the Irish Research Council, and Science Foundation Ireland for financial support.

## ■ REFERENCES

- (1) (a) Yeung, C. S.; Dong, V. M. *Chem. Rev.* **2011**, *111*, 1215–1292. (b) Van Leeuwen, P. W. N. M. *Homogenous Catalysis Understanding the Art*; Kluwer Academic Publishers: Dordrecht, The Netherlands, 2004. (c) Hartwig, J. F. *Organotransition Metal Chemistry, From Bonding to Catalysis*; University Science Books: Sausalito, CA, 2010. (d) van Leeuwen, P. W. N. M.; Chadwick, J. C. *Homogeneous Catalysis: Activity - Stability - Deactivation*; Wiley-VCH: Weinheim, Germany, 2011.
- (2) (a) Seeman, J. I. *Chem. Rev.* **1983**, *83*, 83–134. For a classic example, see: (b) Noyori, R.; Ikeda, T.; Ohkuma, T.; Widhalm, M.; Kitamura, M.; Takaya, H.; Akutagawa, S.; Sayo, N.; Saito, T.; Taketomi, T.; Kumobayashi, H. *J. Am. Chem. Soc.* **1989**, *111*, 9134–9135.
- (3) For a themed issues on ligand non-innocence, see: Hindson, K.; de Bruin, B. *Eur. J. Inorg. Chem.* **2012**, *2012*, 340–342.
- (4) (a) Chirik, P. J.; Wieghardt, K. *Science* **2010**, *327*, 794–795. (b) Kaim, W.; Schwederski, B. *Coord. Chem. Rev.* **2010**, *254*, 1580–1588. (c) Chirik, P. J. *Inorg. Chem.* **2011**, *50*, 9737. (d) Luca, O. R.; Crabtree, R. H. *Chem. Soc. Rev.* **2013**, *42*, 1440–1459.
- (5) For selected examples, see: (a) Legzdins, P.; Rempel, G. L.; Wilkinson, G. J. *Chem. Soc. D* **1969**, 825–825. (b) Rau, S.; Büttner, T.; Temme, C.; Ruben, M.; Görls, H.; Walther, D.; Duati, M.; Fanni, S.; Vos, J. G. *Inorg. Chem.* **2000**, *39*, 1621–1624. (c) Barigelli, F.; Flamigni, L.; Calogero, G.; Hammarström, L.; Sauvage, J.-P.; Collin, J.-P. *Chem. Commun.* **1998**, 2333–2334. (d) Rillema, D. P.; Meyer, T. J.; Conrad, D. *Inorg. Chem.* **1983**, *22*, 1617–1622. (e) Di Pietro, C.; Serroni, S.; Campagna, S.; Gandolfi, M. T.; Ballardini, R.; Fanni, S.; Browne, W. R.; Vos, J. G. *Inorg. Chem.* **2002**, *41*, 2871–2878. (f) Tannai, H.; Tsuge, K.; Sasaki, Y. *Inorg. Chem.* **2005**, *44*, 5206–5208.
- (6) (a) Lebeau, E. L.; Binstead, R. A.; Meyer, T. J. *J. Am. Chem. Soc.* **2001**, *123*, 10535–10544. (b) Huynh, M. H. V.; Meyer, T. J. *Chem. Rev.* **2007**, *107*, 5004–5064. (c) Weinberg, D. R.; Gagliardi, C. J.; Hull, J. F.; Murphy, C. F.; Kent, C. A.; Westlake, B. C.; Paul, A.; Ess, D. H.; McCafferty, D. G.; Meyer, T. J. *Chem. Rev.* **2012**, *112*, 4016–4093.

- (7) Noyori, R.; Hashiguchi, S. *Acc. Chem. Res.* **1997**, *30*, 97–102.
- (8) (a) Gunanathan, C.; Ben-David, Y.; Milstein, D. *Science* **2007**, *317*, 790–792. (b) Kohl, S. W.; Weiner, L.; Schwartsburd, L.; Konstantinovski, L.; Shimon, L. J. W.; Ben-David, Y.; Iron, M. A.; Milstein, D. *Science* **2009**, *324*, 74–77. (c) Milstein, D. *Top. Catal.* **2010**, *53*, 915–923.
- (9) For selected examples, see: (a) Ashby, M. T.; Halpern, J. *J. Am. Chem. Soc.* **1991**, *113*, 589–594. (b) Chu, H. S.; Lau, C. P.; Wong, K. Y.; Wong, W. T. *Organometallics* **1998**, *17*, 2768–2777. (c) Noyori, R.; Ohkuma, T. *Angew. Chem., Int. Ed.* **2001**, *40*, 40–73. (d) Chaplin, A. B.; Dyson, P. J. *Inorg. Chem.* **2008**, *47*, 381–390.
- (10) See for example: Gloaguen, Y.; Rebreyend, C.; Lutz, M.; Kumar, P.; Huber, M.; van der Vlugt, J. I.; Schneider, S.; de Bruin, B. *Angew. Chem., Int. Ed.* **2014**, *53*, 6814–6818.
- (11) Pyridylideneamides are related to pyridylideneamines that have been studied slightly more; see: (a) Doster, M. E.; Johnson, S. A. *Angew. Chem., Int. Ed.* **2009**, *48*, 2185–2187. (b) Shi, Q.; Thatcher, R. J.; Slattery, J.; Sauari, P. S.; Whitwood, A. C.; McGowan, P. C.; Douthwaite, R. E. *Chem. - Eur. J.* **2009**, *15*, 11346–111360. (c) Doster, M. E.; Hatnean, J. A.; Jeftic, T.; Modi, S.; Johnson, S. A. *J. Am. Chem. Soc.* **2010**, *132*, 11923–11925. (d) Doster, M. E.; Johnson, S. A. *Organometallics* **2013**, *32*, 4174–4184.
- (12) For leading general references on N-heterocyclic carbene complexes, see: (a) Nolan, S. P., Ed. *N-Heterocyclic Carbenes*; Wiley-VCH: Weinheim, Germany, 2014. (b) Bourissou, D.; Guerret, O.; Gabbai, F. P.; Bertrand, G. *Chem. Rev.* **2000**, *100*, 39–92. (c) Arnold, P. L.; Pearson, S. *Coord. Chem. Rev.* **2007**, *251*, 596–609. (d) Hahn, F. E.; Jahnke, M. C. *Angew. Chem., Int. Ed.* **2008**, *47*, 3122–3172. (e) Arduengo, A. J.; Bertrand, G. *Chem. Rev.* **2009**, *109*, 3209–3210. (f) Melaimi, M.; Soleilhavoup, M.; Bertrand, G. *Angew. Chem., Int. Ed.* **2010**, *49*, 8810–8849. (g) Benhamou, L.; Chardon, E.; Lavigne, G.; Bellemin-Laponnaz, S.; Cesar, V. *Chem. Rev.* **2011**, *111*, 2705–2733.
- (13) (a) According to the IUPAC Golden Book, mesoionic compounds are “Dipolar five- (possibly six-) membered heterocyclic compounds in which both the negative and the positive charge are delocalized, for which a totally covalent structure cannot be written, and which cannot be represented satisfactorily by any one polar structure. The formal positive charge is associated with the ring atoms, and the formal negative charge is associated with ring atoms or an exocyclic nitrogen or chalcogen atom. Mesoionic compounds are a subclass of betains”: IUPAC. *Compendium of Chemical Terminology*, 2nd ed. (the “Gold Book”); McNaught, A. D.; Wilkinson, A., Eds.; Scientific Publications: Blackwell Oxford, UK, 1997. Formally, PYAs are therefore not mesoionic, since a neutral resonance structure can be drawn. However, we will use this term throughout this article to acknowledge the resonance conjugation of the charges, while alternative terms (such as zwitterionic) insinuate a more localized positive and negative charge. See also: (b) Araki, S.; Wanibe, Y.; Uno, F.; Morikawa, A.; Yamamoto, K.; Chiba, K.; Butsugan, Y. *Chem. Ber.* **1993**, *126*, 1149–1155.
- (14) For leading reviews, see: (a) Cavell, K. J.; McGuinness, D. S. *Coord. Chem. Rev.* **2004**, *248*, 671–681. (b) Crudden, C. M.; Allen, D. P. *Coord. Chem. Rev.* **2004**, *248*, 2247–2273. (c) Kantchev, E. A. B.; O’Brien, C. J.; Organ, M. G. *Angew. Chem., Int. Ed.* **2007**, *46*, 2768–2813. (d) Vougioukalakis, G. C.; Grubbs, R. H. *Chem. Rev.* **2010**, *110*, 1746–1787. For selected recent examples, see: (e) Woods, J. A.; Lalrempuia, R.; Petronilho, A.; McDaniel, N. D.; Müller-Bunz, H.; Albrecht, M.; Bernhard, S. *Energy Environ. Sci.* **2014**, *7*, 2316–2328. (f) Keske, E. C.; Zenkina, O. V.; Wang, R.; Crudden, C. M. *Organometallics* **2012**, *31*, 456–461. (g) Wright, J. R.; Young, P. C.; Lucas, N. T.; Lee, A.-L.; Crowley, J. D. *Organometallics* **2013**, *32*, 7065–7076. (h) Bolje, A.; Hohloch, S.; Urankar, D.; Pevec, A.; Gazvoda, M.; Sarkar, B.; Kosmrlj, J. *Organometallics* **2014**, *33*, 2588–2598. (i) Canseco-Gonzalez, D.; Petronilho, A.; Müller-Bunz, H.; Ohmatsu, K.; Ooi, T.; Albrecht, M. *J. Am. Chem. Soc.* **2013**, *135*, 13193–13203. (j) Heath, R.; Müller-Bunz, H.; Albrecht, M. *Chem. Commun.* **2015**, *51*, 8699–8701. (k) Bagh, B.; McKinty, A.; Lough, A. J.; Stephan, D. W. *Dalton Trans.* **2015**, *44*, 2712–2723.
- (15) For application of NHC complexes in materials, see for example: (a) Boydston, A. J.; Bielawski, C. W. *Dalton Trans.* **2006**, 4073–4077. (b) Mercks, L.; Albrecht, M. *Chem. Soc. Rev.* **2010**, *39*, 1903–1912. (c) Conrady, F. M.; Fröhlich, R.; Schulte to Brinke, C.; Pape, T.; Hahn, F. E. *J. Am. Chem. Soc.* **2011**, *133*, 11496–11499. (d) Schulze, B.; Schubert, U. S. *Chem. Soc. Rev.* **2014**, *43*, 2522–2571.
- (16) For application in medicinal chemistry, see for example: (a) Oehninger, L.; Rubbiani, R.; Ott, I. *Dalton Trans.* **2013**, *42*, 3269–3284. (b) Ott, I. *Coord. Chem. Rev.* **2009**, *253*, 1670–1681. (c) Berners-Price, S. J.; Filipovska, A. *Metallomics* **2011**, *3*, 863–873.
- (17) Boyd, P. D. W.; Wright, L. J.; Zafar, M. N. *Inorg. Chem.* **2011**, *50*, 10522–10524.
- (18) Thatcher, R. J.; Johnson, D. G.; Slattery, J. M.; Douthwaite, R. E. *Chem. - Eur. J.* **2012**, *18*, 4329–4336.
- (19) Slattery, J.; Thatcher, R. J.; Shi, Q.; Douthwaite, R. E. *Pure Appl. Chem.* **2010**, *82*, 1663–1672.
- (20) Leigh, V.; Carleton, D. J.; Olguin, J.; Müller-Bunz, H.; Wright, L. J.; Albrecht, M. *Inorg. Chem.* **2014**, *53*, 8054–8060.
- (21) McGuinness, D. S.; Cavell, K. J. *Organometallics* **2000**, *19*, 741–748.
- (22) (a) Mathew, P.; Neels, A.; Albrecht, M. *J. Am. Chem. Soc.* **2008**, *130*, 13534–13535. (b) Guisado-Barrios, G.; Bouffard, J.; Donnadieu, B.; Bertrand, G. *Angew. Chem., Int. Ed.* **2010**, *49*, 4759–4762. (c) Donnelly, K. F.; Petronilho, A.; Albrecht, M. *Chem. Commun.* **2013**, *49*, 1145–1159. (d) Crowley, J. D.; Lee, A.-L.; Kilpin, K. J. *Aust. J. Chem.* **2011**, *64*, 1118–1132.
- (23) (a) Kolb, H. C.; Finn, M. G.; Sharpless, K. B. *Angew. Chem., Int. Ed.* **2001**, *40*, 2004–2021. (b) Bock, V. D.; Hiemstra, H.; van Maarseveen, J. H. *Eur. J. Org. Chem.* **2006**, *2006*, 51–68. (c) Moses, J. E.; Moorhouse, A. D. *Chem. Soc. Rev.* **2007**, *36*, 1249–1262. (d) Hein, J. E.; Fokin, V. V. *Chem. Soc. Rev.* **2010**, *39*, 1302–1315.
- (24) (a) Keitz, B. K.; Bouffard, J.; Bertrand, G.; Grubbs, R. H. *J. Am. Chem. Soc.* **2011**, *133*, 8498–8501. (b) Poulain, A.; Canseco-Gonzalez, D.; Hynes-Roche, R.; Müller-Bunz, H.; Schuster, O.; Stoekli-Evans, H.; Neels, A.; Albrecht, M. *Organometallics* **2011**, *30*, 1021–1029. (c) Bouffard, J.; Keitz, B. K.; Tonner, R.; Guisado-Barrios, G.; Frenking, G.; Grubbs, R. H.; Bertrand, G. *Organometallics* **2011**, *30*, 2617–2627. (d) Terashima, T.; Inomata, S.; Ogata, K.; Fukuzawa, S. *Eur. J. Inorg. Chem.* **2012**, *2012*, 1387–1393. (e) Yuan, D.; Huynh, H. V. *Organometallics* **2012**, *31*, 405–412. (f) Leigh, V.; Ghattas, W.; Lalrempuia, R.; Müller-Bunz, H.; Pryce, M. T.; Albrecht, M. *Inorg. Chem.* **2013**, *52*, 5395–5402.
- (25) (a) Schuster, O.; Yang, L.; Raubenheimer, H. G.; Albrecht, M. *Chem. Rev.* **2009**, *109*, 3445–3478. (b) Crabtree, R. H. *Coord. Chem. Rev.* **2013**, *257*, 755–766. (c) Albrecht, M. *Adv. Organomet. Chem.* **2014**, *62*, 111–159.
- (26) Kolarovic, A.; Schnuerch, M.; Mihovilovic, M. D. *J. Org. Chem.* **2011**, *76*, 2613–2618.
- (27) The  $pK_a$  of the PYA unit is estimated to be lower than 17, while the  $pK_a$  of triazolium salts is about 25. (a) Bordwell, F. G.; Ji, G. Z. *J. Am. Chem. Soc.* **1991**, *113*, 8398–8401. (b) O’Donoghue, A. M.; Smith, A.; Albrecht, M. Manuscript in preparation.
- (28) Bernet, L.; Lalrempuia, R.; Ghattas, W.; Müller-Bunz, H.; Vigara, L.; Llobet, A.; Albrecht, M. *Chem. Commun.* **2011**, *47*, 8058–8060.
- (29) (a) Cariou, R.; Fischmeister, C.; Toupet, L.; Dixneuf, P. H. *Organometallics* **2006**, *25*, 2126–2128. (b) Clavier, H.; Urbina-Blanco, C. A.; Nolan, S. P. *Organometallics* **2009**, *28*, 2848–2854. (c) Ghattas, W.; Müller-Bunz, H.; Albrecht, M. *Organometallics* **2010**, *29*, 6782–6789. (d) Moret, M.-E.; Chaplin, A. B.; Lawrence, A. K.; Scopelliti, R.; Dyson, P. J. *Organometallics* **2005**, *24*, 4039–4048. (e) Horn, S.; Gandolfi, C.; Albrecht, M. *Eur. J. Inorg. Chem.* **2011**, *2011*, 2863–2868. (f) Gandolfi, C.; Heckenroth, M.; Neels, A.; Laurency, C.; Albrecht, M. *Organometallics* **2009**, *28*, 5112–5121. (g) Kauffhold, O.; Flores-Figueroa, A.; Pape, T.; Hahn, F. E. *Organometallics* **2009**, *28*, 896–901. (h) Flores-Figueroa, A.; Kauffhold, O.; Hepp, A.; Fröhlich, R.; Hahn, F. E. *Organometallics* **2009**, *28*, 6362–6369.
- (30) Abbotto, A.; Bradamante, S.; Pagani, G. A. *J. Org. Chem.* **2001**, *66*, 8883–8892.

(31) Previous work suggested to consider  $\Delta\delta$  as a probe where a large frequency difference suggests a larger influence of local charges and hence a predominant role of the mesoionic structure, refs 20 and 30. A more general descriptor separates the  $\Delta\delta$  into a downfield shift component for the  $\alpha$  proton and an upfield shift component of the  $\beta$  proton, i.e.,  $\Delta\delta = \Delta\delta(\text{H}_\alpha) - \Delta\delta(\text{H}_\beta)$ , as opposed to a simple quantification of  $|\Delta\delta|$ . Even though the spectral data for complex 5 seem at first glance to reduce the chemical shift difference between the two types of pyridine protons upon increasing the polarity, the deshielding and shielding effect for the  $\alpha$  and  $\beta$  protons follows the same trend as observed for 1 and PYE. While in these previously studied compounds the  $\alpha$  protons are more deshielded than the  $\beta$  protons, the sequence is inverted in complex 5, as confirmed by NOE spectroscopy.

(32) Griffiths, T. R.; Pugh, D. C. *Coord. Chem. Rev.* **1979**, *29*, 129–211.

(33) The relatively small difference may not be resonance structure dependent but just reflect the increased stability of a ruthenium(III) complex in more polar solvents. An unambiguous comparison with complex 7, which cannot undergo a similar resonance structure modification, was prevented, as the oxidation of this complex in MeNO<sub>2</sub> was irreversible. The difference in oxidation potential was similar however, with an  $E_{\text{pa}}$  at +1.39 V in MeNO<sub>2</sub> vs an  $E_{\text{pa}}$  at +1.47 V in CH<sub>2</sub>Cl<sub>2</sub>.

(34) Traore, H.; Saunders, M.; Blasiman. *Aust. J. Chem.* **2000**, *53*, 951–957.

(35) For related NHC ruthenium complexes in transfer hydrogenation catalysis, see: (a) Poyatos, M.; Mata, J. A.; Falomir, E.; Crabtree, R. H.; Peris, E. *Organometallics* **2003**, *22*, 1110–1114. (b) Burling, S.; Whittlesey, M. K.; Williams, J. M. J. *Adv. Synth. Catal.* **2005**, *347*, 591–594. (c) Poyatos, M.; Maise-Francois, A.; Bellemin-Laponnaz, S.; Peris, E.; Gade, L. H. *J. Organomet. Chem.* **2006**, *691*, 2713–2720. (d) Fekete, M.; Joo, F. *Collect. Czech. Chem. Commun.* **2007**, *72*, 1037–1045. (e) Prades, A.; Viciano, M.; Sanau, M.; Peris, E. *Organometallics* **2008**, *27*, 4254–4259. (f) Sanz, S.; Azua, A.; Peris, E. *Dalton Trans.* **2010**, *39*, 6339–6343. (g) Burling, S.; Paine, B. M.; Nama, D.; Brown, V. S.; Mahon, M. F.; Prior, T. J.; Pregosin, P. S.; Whittlesey, M. K.; Williams, J. M. J. *J. Am. Chem. Soc.* **2007**, *129*, 1987–1995.

(36) A similar effect of DMA was also noted when using cyclohexanone as substrate. However, the reaction was much faster (full conversion within 2 h), and accordingly, the trends were less pronounced.

(37) Delgado-Rebollo, M.; Canseco-Gonzalez, D.; Hollering, M.; Mueller-Bunz, H.; Albrecht, M. *Dalton Trans.* **2014**, *43*, 4462–4473.

(38) The different solvent dependence of complexes 5 and 7 also indicates that chloride dissociation or substitution is not responsible for the diverging response to DMA addition, since chloride solvation should be equal for both complexes.

(39) (a) Prades, A.; Peris, E.; Albrecht, M. *Organometallics* **2011**, *30*, 1162–1167. (b) Canseco-Gonzalez, D.; Albrecht, M. *Dalton Trans.* **2013**, *42*, 7424–7432. (c) Bagh, B.; McKinty, A.; Lough, A. J.; Stephan, D. W. *Dalton Trans.* **2014**, *43*, 12842–12850.

(40) Kuhlman, R.; Streib, W. E.; Huffman, J. C.; Caulton, K. G. *J. Am. Chem. Soc.* **1996**, *118*, 6934–6945.

(41) Connelly, N. G.; Geiger, W. E. *Chem. Rev.* **1996**, *96*, 877–910.

(42) Clark, R. C.; Reid, J. S. *Acta Crystallogr., Sect. A: Found. Crystallogr.* **1995**, *A51*, 887–897.

(43) Sheldrick, G. M. *Acta Crystallogr., Sect. A: Found. Crystallogr.* **2008**, *A64*, 112–122.